

TEKNOFEST

**AVIATION, SPACE AND TECHNOLOGY
FESTIVAL**

**UNMANNED UNDERWATER SYSTEMS
COMPETITION**

CRITICAL DESIGN REPORT

EVA ROV

SENIOR CATEGORY

APPLICATION ID: 377724



CONTENTS

1. REPORT SUMMARY	3
2. TEAM CHART.....	3
3. PROJECT CURRENT STATUS ASSESSMENT	4
4. VEHICLE DESIGN	4
5. SAFETY	20
6. TESTS	21
7. EXPERIENCES.....	22
8. TIME, BUDGET, AND RISK PLANNING.....	23
9. ORIGINALITY	24
10. DOMESTIC COMPONENTS.....	27
11. REFERENCES	30



The EVA ROV Team's Critical Design Report includes mechanical, electronic and software parts. System design, production and development processes are mentioned. There were no major changes from the Preliminary Design Report. Since the thrusters, hydrophones, motor drivers, batteries, AUV recovery system, power distribution board were all designed and manufactured on time as planned previously.

Manufactured by EVA ROV Team, the AUV called Saturn is equipped with 6 powerful thrusters and sensors such as a stereo camera are placed. In addition, while processing movement algorithms and data from all these sensors with the NVIDIA Jetson Xavier NX Developer Kit, it also made Saturn a fully autonomous vehicle thanks to the artificial intelligence integration trained by the EVA ROV Team. It is designed to perform the tasks with computer vision and acoustic sensing.

Four original hydrophones are produced by EVA ROV Team in order to carry out the third mission of the competition. In addition, the motor, motor driver and battery are produced domestically and originally by EVA ROV Team.

Every detail of the design process, which was briefly mentioned in the report summary section, was conveyed to the reader in the report.

EVA ROV Team consists of 1 PhD level project advisor and 10 undergraduate level members. There are 4 mechanical team members, 3 software team members, 2 electrical team members and 1 management team member. Team chart is presented in Figure 2.1.



3. PROJECT CURRENT STATUS ASSESSMENT

EVA ROV Team's Preliminary Design Report, which was sent for the application made to the Unmanned Underwater Systems Senior Category of the TEKNOFEST 2022 competition, was evaluated by expert referees and scored 85 points out of 100 points. After the evaluation of the Preliminary Design Report, the points that lost points were determined and carefully examined. As a result of these examinations, some changes were made to the report format.

After the preliminary design report, the mechanical and electronic equipment of the vehicle remained mostly the same, only minor changes were made. The production and assembly stages of these changes are nearing the end. In this process, emphasis was placed on testing and software development. With the announcement of the technical drawings of the competition tracks, the production of the track started. With the tracks completed in a short time, work on image processing began. Pool tests were increased to detect and perform software adjustments.

3.1. Changes Made with The Report Format and Their Reasons

As a result of the evaluations, we decided that the team summary and team chart were insufficient, so we detailed them. We provided more information about team members.

3.2 Changes Made to The Vehicle and Their Reasons

In the PDR, it is said that ZED 2 as a camera will be used. Instead of that, it is decided to use the ZED Mini camera, which takes up less space. Thanks to this, there is more space for other components. Studies about OpenCV is continuing to detect the circles' colors in Task 1. In addition, using Sea Thru algorithm is decided to make underwater colors more vivid and to contribute to image processing. Further information about Sea Thru algorithm is presented in Section 4.2.3. Moreover, GPS system is added in order to be aware of the AUV's location in case the battery of the AUV runs out while using a solar panel.

3.3 Difference Between Preliminary Design Report and Critical Design Report

The cost of the vehicle increased due to the change in the materials that the team had previously agreed on and the increase in the exchange rate difference. The budget comparison is presented in Table 3.1.

Table 3.1. Budget Comparison.

	The Preliminary Design Report	The Critical Design Report
Cost of Materials	₺ 40.000	₺ 50.000
Production Cost	₺4.800	₺5.000
Total Budget	₺ 44.800	₺ 55.000

4. VEHICLE DESIGN

4.1. System Design

The system design plan of EVA ROV Team is presented in Figure 4.1.

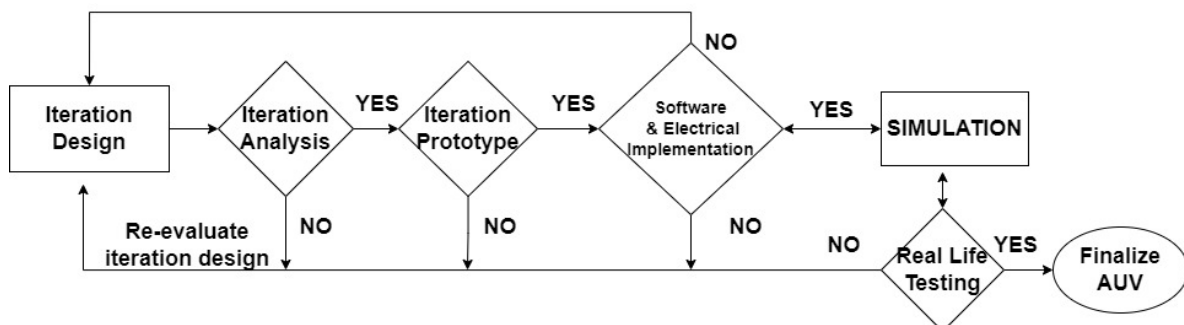


Figure 4.1 EVA ROV Team System Design Plan.

4.1.1. Mechanical Design of the Vehicle

During the mechanical design phase, a plan was made to specify all the necessary needs and precautions required to design an optimized AUV body which fits the needs and is compatible with all the systems in the vehicle, in order to efficiently execute the required missions, while taking into consideration the real-world application. A thorough research has been done to develop the conceptual design of the vehicle, considering the mechanical aspects and the prerequisites of the other systems. The most crucial domains were defined as the following: pressure resistance, hydrodynamic, movement precision, dimensions, weight, and interior space. The design process includes the body, shell, tray, motors, and propellers.

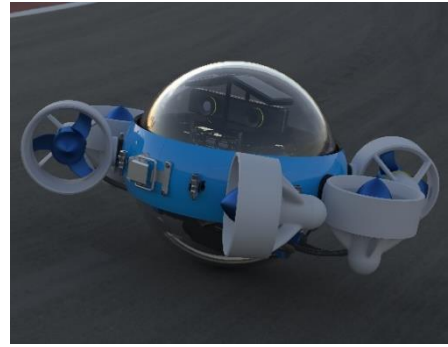


Figure 4.0 “Saturn” render

4.2.1.1 Body Design Process

For the design process of the body, the idea starts as a concept, that gets developed into a technical drawing using SOLIDWORKS, that gets refined on Fusion360 and 3D printed, ANSYS was also implemented before any design was finalized to understand and compare how the AUV will function underwater, for designing the propellers PropCad2021 was used.

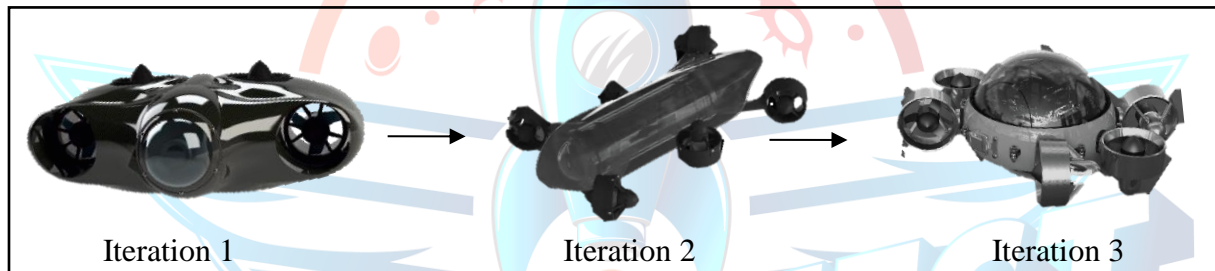


Figure 4.1 Iterations Designs.

As illustrated in Figure 4.2, the first iteration was considered, in which the tube is enclosed by a PLA body and four thrusters are situated within tunnels to optimize the thrusters' performance. With this design, we struggled with the amount of space available within the tube, as most of the body is made of PLA and the electrical components must only fit along the tube. Furthermore, since this design relies on four motors, the AUV will require a greater amount of thrust in order to move. Due to the variable nature of the competition's tasks, the bouncing of such a device cannot be regulated within the stipulated weight. The second iteration was developed in response to the issues identified in the first iteration. To enhance the amount of force required to propel the AUV, two additional thrusters were installed and the direction was altered. Moreover, the tube occupied the major portion of the design area where the components would be housed. Finally, landing back on the spherical shape that will be used in the competition, it gives the advantage of being sufficiently symmetrical, it also occupies the same volume of space as it turns,



Figure 4.2 Iteration 1 Final Design.

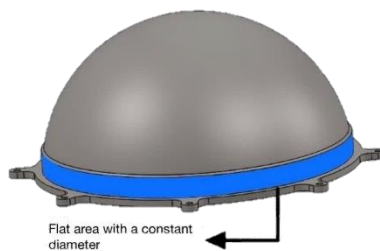


Figure 4.3 Upper Dome.



Figure 4.4 Bottom Dome.

which facilitates maneuverability in confined spaces and small targets [1], as is the case in real-world applications such as the ocean and competition activities. In addition, the volume of a spherical form offers us with more free space than virtually any other shape, allowing us to store electrical components and sensors inside the body. Adding attachments (such as robotic arms or a payload) is as well simple since the outer shell can be modified as desired. Due to its zero-degree turn radius, its performance in rotations is further enhanced. A spherical shape has a low coefficient of drag due to its symmetrical orientation, consistent fluid dynamic computations, and constant hydrodynamic parameters [2]. The main body consists of two domes made of plexiglass mounted together to house all the electrical components; both have an outer diameter of 224 mm with a thickness of 5 mm. A radial aluminum flange with two grooves was adopted as a sealing method for the AUV, as a result some amendments were made for domes to be consistent with the selected method. As shown in Figure 4.3, the domes include an area with a constant diameter as a housing for the flange. The two domes will be assembled with eight M5 screws to ensure a tightly closed body.

Penetrators were chosen as an intermediary for the wires to pass through the body, however, it is not screwable in a curved shape so, a flat area was required to place the penetrators, accordingly, a rectangular like-shape with an arc, was cut and made for the bottom dome from each side with 12 holes having a diameter of 10 mm as shown in Figure 4.4 penetrators are sealed by using a waterproof epoxy.



Figure 4.5 Shell Design 3D View.

The body is enclosed with a PLA shell that holds the six thrusters as well as providing the essential protection and ensuring the two domes are linked. it is divided into two parts to fit around the spherical shape, and it is merged by using a latch from each side. The shell is adjustable and may house extra elements depending on the mission, such as acoustic system components. It has a sphere - like form that is meant to fit the body's hydrodynamics

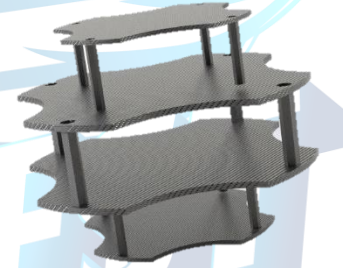


Figure 4.6 Electronics Tray Design.

The tray geometry is tailored to match the contours of the body. It is made up of four separate plates that are spaced apart by a distance that encompasses all the components. Taking into consideration the convenience with which wires can be supplied and the excellent organization that exists inside the body, which makes the process of maintenance more manageable, since carbon fiber is electrically conductive, an epoxy layer was added to make sure that it insulates , Figure 4.21 shows the new technical drawing of the AUV with a smaller overall diameter and lower thickness to easy up the manufacturing process.

4.2.2. Materials

The shell of the body was manufactured with plexiglass, due to its neutral density , and shatter resistance compared to glass , PLA & ABS were considered, but since they don't offer the added benefits of transparency , that wouldn't allow solar panels to be installed inside the AUV , while allowing easy identification of hardware failure or water leakage, A non-dimensional value k is defined through calculating the stress through dividing the critical buckling stress, where the value of k would show the margin of the shell instability resistance ,

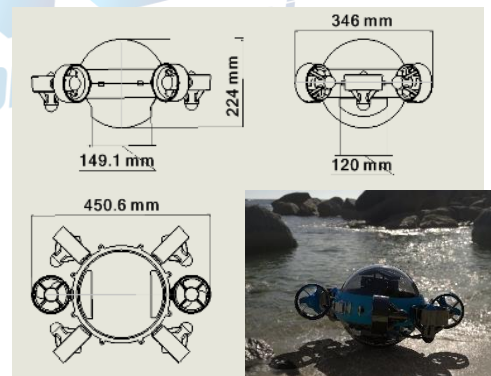


Figure 4.11 AUV Technical Drawing.

if $k < 1$ it means that the shell wouldn't be stable, based on that, the shell thickness was calculated and picked as 5mm to make sure that the shell remains stable, and since increasing the shell thickness increases the k [3], therefore insures a stable underwater static pressure, The Critical stress P_{cr} was found as 3.91Mpa which means that the shell shall withstand a depth of more than 390m underwater

$$p_{cr} = \frac{2}{\sqrt{3(1-\mu^2)}} E \frac{t^2}{R^2} \left(-e^2 + \frac{1}{10}e + 1 \right)$$

$p_{cr} = \frac{2}{\sqrt{3(1-\mu^2)}} E \frac{t^2}{R^2} = 3.91\text{MPa}$

R surface radius.

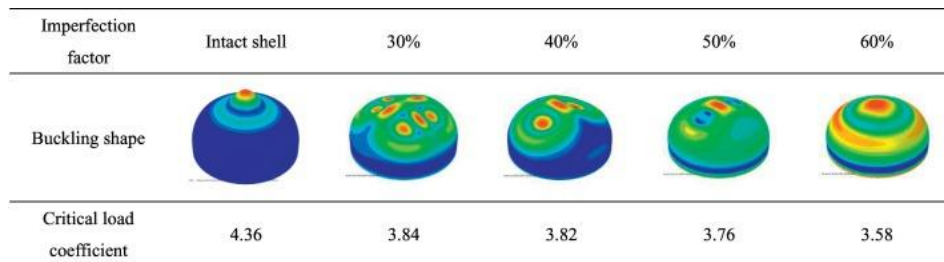


Figure 4.7 Critical Load Coefficient Range With Imperfection Factor.

The inner plate holding the components inside the AUV was made from carbon fiber due to its light weight and flex resistance. A lead weight was designed to be placed at the bottom of the AUV Due to its very high destiny, in order to shift the center of mass downwards without compromising the inner space of the body.

Table 4.2 Material List.

Material	specifications	Density	Usage
Plexi glass	Transparency Breakage, Shatter resistant Weather Resistance Heat Formable Light Weight Heat resistance (180-200 F)	1.18gm/cm ³	Outer AUV Body
Carbon fiber	Physical strength, specific toughness, light weight, good vibration damping, strength, and toughness, High dimensional stability, low coefficient of thermal expansion, and low abrasion, biological inertness and x-ray permeability	1.62gm/cm ³	Electronic trays
PLA	High printing accuracy, Good mechanical strength	1.25gm/cm ³	Outer shell
ABS	High rigidity. /Good impact resistance, good insulating properties., Good weldability, good abrasion and strain resistance, High dimensional stability, High surface brightness and excellent surface aspect.	1.05gm/cm ³	Propellor
Polyurethane	High impact resistance, easily processed, and dyed/Excellent water pressure resistance, does not rot under water, does not deform, Suitable for freshwater and saltwater/Compatible with many adhesives	0.20gm/cm ³	AUV floater
Lead	Soft and malleable, has a relatively low melting point, Major advantage of lead shield is in its compactness due to its higher density.	11.3gm/cm ³	Camera Housing box (weight block)

4.2.2.1 Thruster design

The mechanical design of the motors designed using SolidWorks, who's electromagnetic analyses was also completed. Two different type of motors has been designed, rim driven motor was considered, since it produces less acoustic noise, and no pollution since its hydro lubricant, an

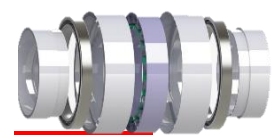


Figure 4.8. Rim Driven Motor Prototype.

also outer runner motor designed. Working prototypes of the designed motors are presented in Figure 4.8. Further Thruster information is given in section 4.2.1.8. ,All the domestic, and purchased components are also explained in detail in section 4.2.1

4.2.3. Production Methods

4.2.3.1. Thermoforming

Thermoforming was used for the domes because it facilitates the creation of a spherical shape at the design's ends and provides a flawless radius transitioning from the straight flange radius. The first step in the process of making a dome out of plexiglass involves heating a piece of acrylic up until it reaches a temperature between 150–160 °C [4]. A mould made of MFD with thickness of 20 mm and 214 mm diameter was made to obtain the specified area for the flange, and it has been placed under the plexiglass sheet. After this step has been completed, the piece of acrylic is ready to be fed into the Dome Blowing device, where it will be secured in place under a circular ring and blown into a dome shape. After that, air pressure is given to the bottom of the acrylic, and it is blown up and out into a uniform dome shape until it achieves the height desired. After it has been allowed to cool down, it may be released from the circular clamp. One of the domes was then taken and a pair of rectangular-like incisions were made, as well as holes for the wires, then being reattached to the dome using waterproof silicon as presented in Figure 4.8.



Figure 4.8. Dome Manufacturing.

4.2.3.3. Vacuum Infusion

Vacuum Infusion was used for the carbon fiber tray because it provides the strongest structure for a low number of layers. We also used prepreg carbon fiber, so vacuuming it before putting it in the oven gave us a great finished surface and a strong structure after it was manufactured. The tray is comprised of prepreg carbon fiber, as previously stated. To make the core material, six layers of prepreg carbon fiber were stacked on top of each other and vacuumed into a rectangular form. After heating it for 6 hours at 45 °C, it was removed from the oven. After the product has cooled, it is now ready for CNC cutting to the desired shape. This process shown in Figure 4.9.

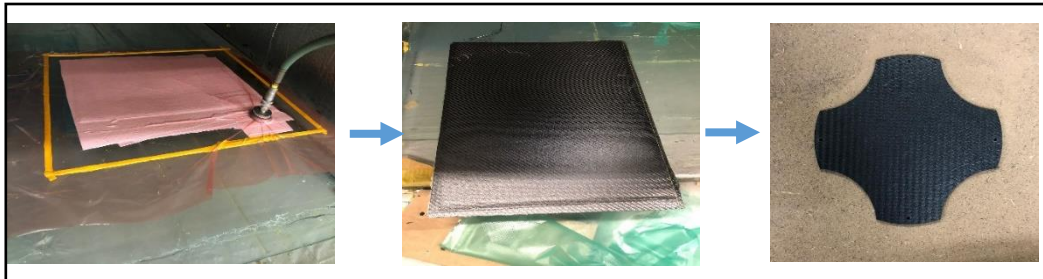


Figure 4.9 Electronics Tray Manufacturing Process.

4.2.3.3. CNC-Cutting

In comparison to alternative cutting equipment, such as water jet cutting, CNC cutting was chosen because it is widely accessible and inexpensive, shown in the Figure 4.9, the ready prepreg

carbon fiber block will be machined into three trays. When it comes to the flange, it was designed it on SOLIDWORKS with the necessary calculations to ensure that it is equivalent to the standard and a technical drawing was prepared then a T-6 7075 Aluminium was CNC-cut accordingly.

4.2.3.4. 3D Printing

3D printing was chosen all of our plastic parts that has been used in our AUV since it is inexpensive and easily accessible, the plastic parts were designed on SOLIDWORKS as needed, taking into consideration how it would affect the design. And later on printed usually with a 100 percent filling to ensure it sturdiness and resistant to the forces it would withstand.

4.2.4. Physical Properties

After the PDR, some changes were made for the dimension of the vehicle. Due to difficulties in manufacturing, some aspects of the design had to be changed without it effecting its performance. To have good control of buoyancy and to ensure the AUV's easy mobility some specified areas had to be considered whether to add an additional weight or foam to adjust the bouncy the total weight of the AUV foams is deployed as floaters in a certain location to achieve the appropriate buoyancy

Table 4.2 Mass Budget List

Type	Quantity	Mass (kg)	Total mass (kg)
G-350	6	0.28	1.68
ECS	6	0.035	0.21
Aluminum Flange	1	0.46	0.46
PLA shell	1	0.32	0.32
PLA Tray	1	0.436	0.436
Jetson NX	1	0.1772	0.1772
Battery	1	0.603	0.603
Custom Power Distribution	1	0.024	0.024
Penetrator	6	0.026	0.156
Zed Mini Camera	1	0.062	0.062
Pressure Sensor	1	0.026	0.026
Switch	1	0.026	0.026

Type	Quantity	Mass (kg)	Total Mass (kg)
Pixhawk	1	0.04	0.04
STM	1	0.063	0.063
Solar Panel	2	0.10	0.20
Upper Plexiglass Dome	1	0.658	0.658
Bottom Plexiglass Dome	1	0.73	0.73
Servo Motor	1	0.023	0.023
Hydrophones	4	0.022	0.088
Light	1	0.165	0.165
Latch	2	0.040	0.080
Total			6.2272
Weight in Air (N)			61.088832

Table 4.3 Buoyancy calculations

Type	Quantity	Total Volume (m ³)	Buoyancy Force (N)	Total Weight of AUV (N)	Net Force (N)
G-350 thruster	6	0.000912	8.947	-	-
Upper dome	1	0.002981	29.244	-	-
Bottom dome	1	0.002845	27.909	-	-
Shell	1	0.000232	2.276	-	-
Total		0.00697	68.376	61.088832	7.287168

The buoyancy calculations yielded a net force of roughly 7.29N, allowing our AUV to maintain a semi-neutral buoyancy once placed in water, as shown in Table 4.5

4.2.1. Electronic Design Process

Description of the electronic system, including the original and domestically produced components by EVA ROV Team, is presented in this section. Electronic design schematic of Saturn is presented in Figure 4.12.

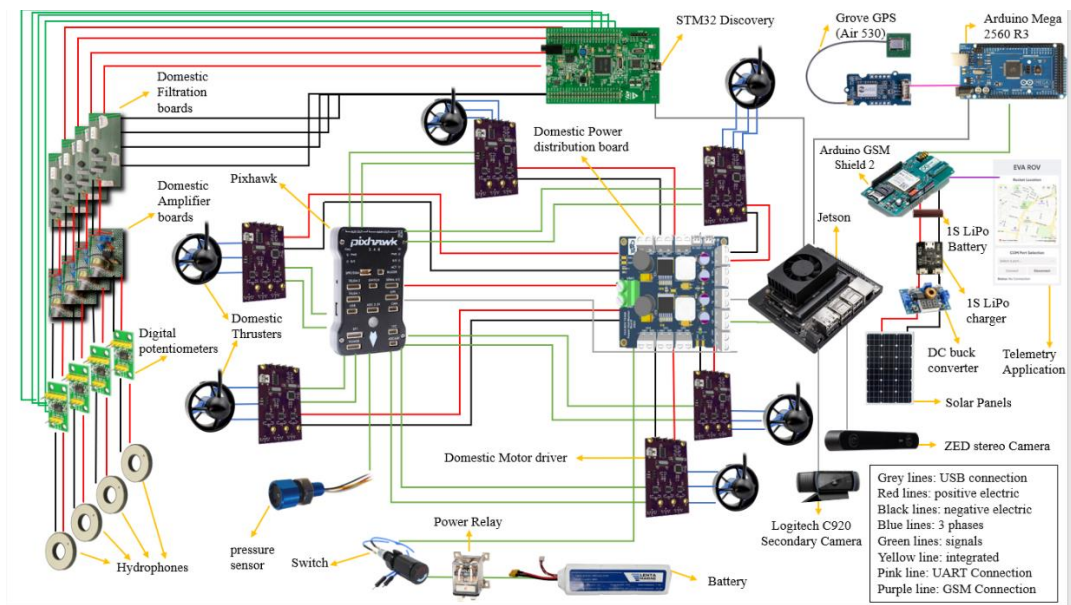


Figure 4.12 Electronic Design.

4.2.1.1. Autopilot Card

Saturn's autopilot card, Pixhawk PX4, is one of the main components of the system where ArduSub software is loaded. The Pixhawk device allows using the vehicle autonomously by using ArduSub library via Python. Pixhawk device primarily acts as a bridge between the companion computer and the tools. The reason of using Pixhawk PX4 as autopilot card is the way it offers real-time operation and high-performance signal processing with a low delay while compacting a light.



Figure 4.13
Pixhawk PX4.

4.2.1.2. Companion Computer

The companion computer is connected to the autopilot board. It routes and processes data using the MavLink protocol, which is Router is used to route telemetry between the companion computers serial port and any network endpoints. Mainly, companion computer has two main functions. These are streaming HD video to the host and providing communication between the autopilot card and the host computer via Ethernet.

NVIDIA Jetson Xavier NX Developer Kit –shown in Figure 4.14 - is used as the control center. According to EVA ROV Team's previous experiences, it was determined that it is a suitable single board computer for image processing. The reason of using NVIDIA Jetson Xavier NX is the way it provides deep learning methods and AUV control, due to its NVIDIA Volta architecture with 384 NVIDIA CUDA cores and 48 Tensor cores. Also NVIDIA Jetson Xavier NX delivers up to 21 TOPS for running modern AI workloads.



Figure 4.14 NVIDIA
Jetson Xavier NX.

4.2.1.3. Dual Camera System

In AUV, ZED Mini stereo camera – shown in Figure 4.15 - is used for object detection system. ZED Mini stereo camera is a camera that simulates both eyes and human vision. This camera senses its surroundings through triangulation and creates a three-dimensional model of

the scene. First of all, it synchronizes the image it receives from both cameras on the ZED Mini stereo camera. These images are used by the ZED software and output a depth map. With the help of this depth map or by obtaining a 3D point cloud, the distance of objects to the camera can be calculated. It has fast 2K image sensors and a 110-degree field of view (FoV). With an eye-to-eye distance of 63 mm, the camera realizes depth detection from 0.1 meters to 12 meters. The reason for using this camera is that after detecting the objects and obstacles underwater, the distances of the objects and the obstacle are measured and it allows to make a decision with these data. Functional SDK Diagram of ZED SDK is shown in Figure 4.16. Further information about tests held on by EVA ROV Team about depth sensing with stereo camera is presented in Section 6.2.



Figure 4.15. ZED Mini Stereo Camera.

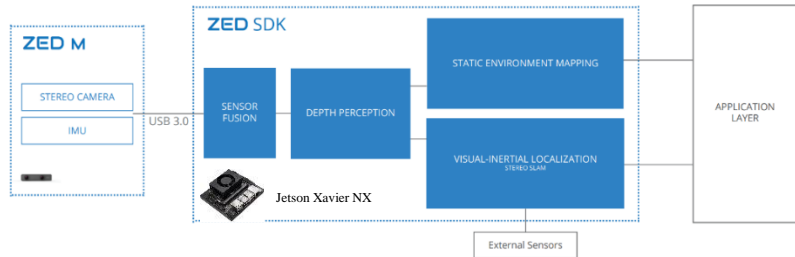


Figure 4.16. Functional SDK Diagram.

A dual camera system has created by EVA ROV Team. Apart from the stereo camera, a Logitech C920 camera is used for use in task 1. The reason for using this camera is to allow the Logitech camera to initialize and start scanning the pool floor after the stereo camera detects the red circle and its distance.

4.3.1.4. Electronic Speed Controller

To create EVA ROV Team's original ESC – shown in Figure 4.17- , 3 main part needed to take into. These are microprocessor, voltage regulation, power and back emf sensing. In microprocessor part, it has an ATMEGA32U4 microprocessor. In the voltage regulation part, it has two voltage regulators these are LM2596 and L7805. LM2596 is used for converting an input voltage to 12 volts these 12 Volt used for switching the MOSFETs. L7805 supply voltage for the microprocessor. On the power side, there are 3 MOSFET drivers and 6 MOSFETs, MOSFET drivers are IR2010 and MOSFETs are 75nf75. In back-emf sensing part, it has a voltage divider and this voltage divider should be configured according to the input voltage and voltage generated by the BLDC motor type because as a back emf comparator used internal comparator of microprocessor and more than 5 volts can damage the microprocessor.

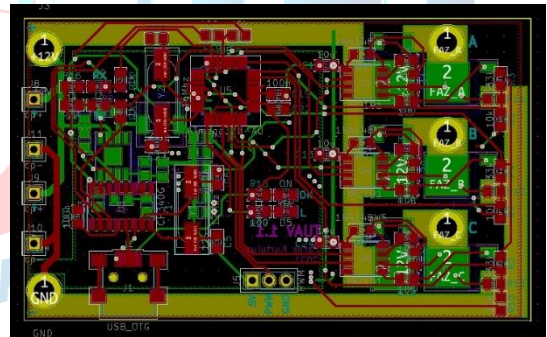


Figure 4.17 Electronic Speed Controller.

4.3.1.4.1 ESC Microprocessor

The reason that selecting ATMEGA32U4 is that it has 6 PWM mode on timer 4. This mode is designed specifically for driving a BLDC motor. With this mode, it can be adjusted easily with complimentary 6 PWM output. Also, can be adjusted the dead time between high side switching and low side switching. The microprocessor also has an internal comparator. It can be sensed back emf of the BLDC motor and with this data by using this microprocessor. It can be decided the commutation step. In addition, this microprocessor is used worldwide, so there are so many sources about this microprocessor. The microprocessor schematic is presented in Figure 4.18.

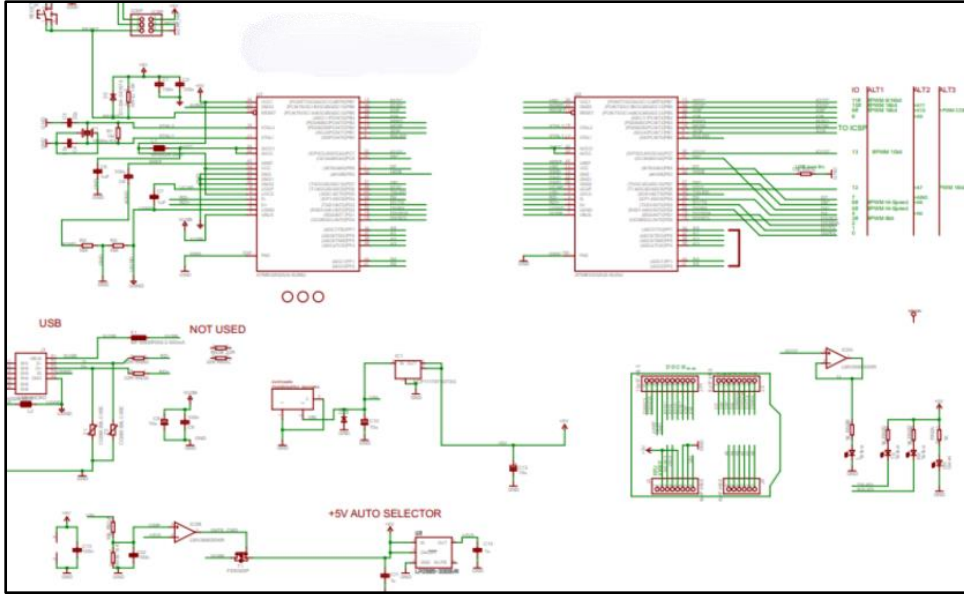


Figure 4.18 Microprocessor Schematic.

4.3.1.4.2 Voltage Regulation

Voltage regulation part uses LM2596 and L7805. These parts supply voltage to the microprocessor and FET Driver IC. LM2596 maximum supply voltage (V_{IN}) is 40 volt, which means it can be 12V to 40 Volt to get 12 Volt output voltage. Schematic of LM2596 is presented in Figure 4.19.

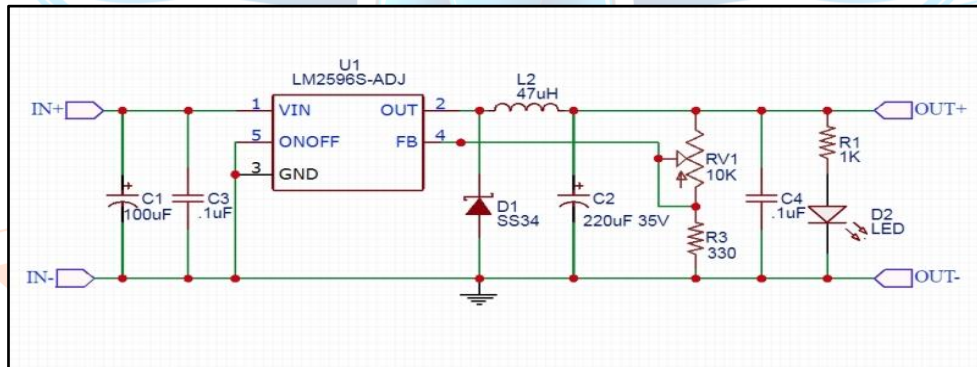


Figure 4.19 Schematic of LM2596

L7805 is IC that call as linear voltage regulator it efficiency is not good as LM2596 but it has do not need extra component to use also it is use for only supply voltage of microprocessor so driving current not too much in this condition for smaller PCB design is has been use. Absolute ratings and some application note taken L7805 datasheets are presented in Figure 4.20.

Symbol	Parameter	Value	Unit
V_I	DC Input Voltage	for $V_O = 5$ to 18V for $V_O = 20, 24V$	V
I_O	Output Current	Internally Limited	
P_{tot}	Power Dissipation	Internally Limited	
T_{stg}	Storage Temperature Range	-65 to 150	$^{\circ}C$
T_{op}	Operating Junction Temperature Range	for L7800 for L7800C	$^{\circ}C$

Absolute Maximum Ratings are those values beyond which damage to the device may occur. Functional operation under these condition is not implied.

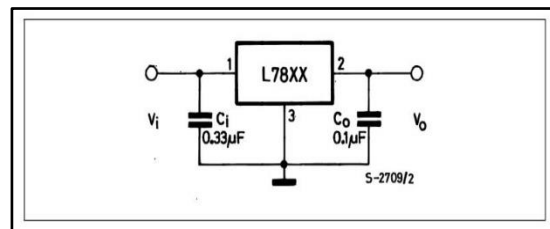


Figure 4.20 Linear Voltage Regulator Datasheet.

4.3.1.4.3 Power

In power section it has 2 N type power MOSFETs for each phase. These MOSFETs connecting as Half H Bridge. MOSFETs maximum voltage ratings (V_{DS}) are 75 volt and maximum drain currents (I_D) are 80 A. These MOSFETs has very low Q_{gate} and exceptional dv/dt capability that means it can turn on and off MOSFET very high speed with that it has very low switching losses. In Figure 4.21 there are important information about MOSFET taken its datasheets.

Symbol	Parameter	Test conditions	Min.	Typ.	Max.	Unit
$g_{fs}^{(1)}$	Forward transconductance	$V_{DS} = 15V, I_D = 40A$		20		S
C_{iss}	Input capacitance	$V_{DS} = 25V, f = 1\text{ MHz}, V_{GS} = 0$		3700		pF
C_{oss}	Output capacitance			730		pF
C_{rss}	Reverse transfer capacitance			240		pF
Q_g	Total gate charge	$V_{DD} = 60V, I_D = 80A$		117	160	nC
Q_{gs}	Gate-source charge	$V_{GS} = 10V$		27		nC
Q_{gd}	Gate-drain charge			47		nC

1. Pulsed: pulse duration=300 μ s, duty cycle 1.5%

Symbol	Parameter	Value		Unit
		D ² PAK / TO-220	TO-220FP	
V_{DS}	Drain-source voltage ($V_{GS} = 0$)	75		V
V_{DGR}	Drain-gate voltage ($R_{DS} = 20K\Omega$)	75		V
V_{GS}	Gate-source voltage	±20		V
$I_D^{(1)}$	Drain current (continuous) at $T_C = 25^\circ\text{C}$	80	80	A
$I_D^{(1)}$	Drain current (continuous) at $T_C = 100^\circ\text{C}$	70	70	A
$I_{DM}^{(2)}$	Drain current (pulsed)	320	320	A
P_{TOT}	Total dissipation at $T_C = 25^\circ\text{C}$	300	45	W
	Derrating factor	2.0	0.3	W/ $^\circ\text{C}$
$dv/dt^{(3)}$	Peak diode recovery voltage slope	12		V/ns
$E_{AS}^{(4)}$	Single pulse avalanche energy	700		mJ
V_{ISO}	Insulation withstand voltage (RMS) from all three leads to external heat sink ($t = 1s, T_C = 25^\circ\text{C}$)	—	2000	V
T_J	Operating junction temperature	-55 to 175		$^\circ\text{C}$
T_{stg}	Storage temperature			

1. Current limited by package
2. Pulse width limited by safe operating area
3. $I_{SD} = 80A, dv/dt < 300A/\mu s, V_{DS} = V_{GSS}, T_J < T_{JMAX}$
4. Starting $T_J = 25^\circ\text{C}, I_D = 40A, V_{DD} = 37.5V$

Figure 4.21 MOSFET Dynamic Data Sheets. **Figure 4.22** Mosfet Absolute Maximum Rating.

Power section Fets driver are IR2010 The IR2010 is a high power, high voltage, high speed power MOSFET and IGBT drivers with independent high and low side referenced output channels. Logic inputs are compatible with standard CMOS or LSTTL output, down to 3.0V logic. The output drivers feature a high pulse current buffer stage designed for minimum driver cross-conduction. Propagation de-lays are matched to simplify use in high frequency applications. The floating channel can be used to drive an N-channel power MOSFET or IGBT in the high side configuration which operates up to 200 volts. Proprietary HVIC and latch immune CMOS technologies enable ruggedized monolithic construction. In Figure 4.21 and Figure 4.22 there are important information about MOSFET driver taken its datasheets.

4.3.1.4.4 Back EMF Sensing

The back EMF sensing has an arrangeable voltage divider made by a resistor. It should be arranged according to the motor and operating voltage value for testing the motor. It has 33k and 10k resistor values. This value can give correct data.

4.3.1.5. Power Sensing Module

It provides analog current and voltage sensing to the autopilot in the vehicle. It allows us to see visual indicators about battery level and current consumption. It connects directly from power supply to the Pixhawk device.

The Power Sensing Module doesn't provide power to the Pixhawk. So it requires a Power Supply. Then Power Sensing Module can be used as a bridge between Power Supply and Pixhawk. So, the main task is sensing voltage, and analog current, and giving information to the users.

4.3.1.6. Power Distribution Board

For the voltage values obtained from the batteries and power station to be used in the system to the appropriate voltage value for the system components, it needs to go through a series of processes. Here, it has included the necessary power distribution card, taking into account the required current value of the active elements that consume power in the system. Power Distribution Board Schematic and 3D Render is presented in Figure 4.23.

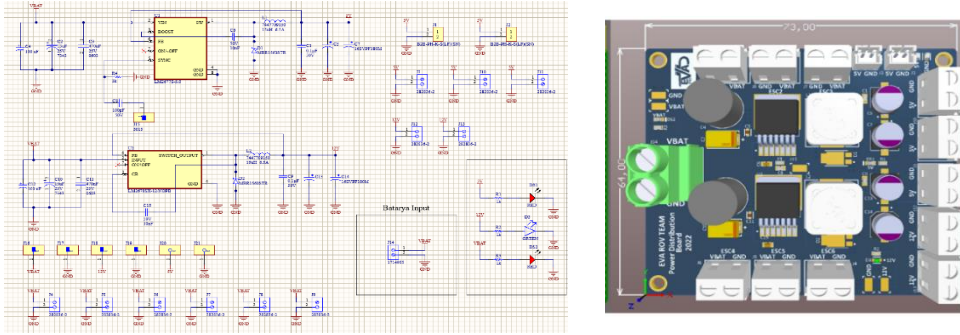


Figure 4.23 Power Distribution Board Schematic and 3D Render.

5S lipo battery is used in the vehicle where a current of 5S, that is, a maximum of 21 volts, will come from the battery. Light, Raspberry Pi, and Pixhawk require 5 volts and a total of 3 amps. For this reason, the LM2677S-5.0/NOPB integrated into the design using Altium. Because this integration has a value of 5 volts and 5 amps, For the Jetson, LM2678SX-12/NOPB has used regulator IC. It was used because it has 12 volts and 5 amps output and the Jetson has an output between 8 and 20 volts and a value of 1.8 amps. Further information is presented in Section 10.1.

4.3.1.7. Battery

Since Saturn weights below 8 kg, the thrusters of AUV doesn't require a thrust power of more than 10KgF to move, therefore a costume domestic there was no need to go above 4S,16v,5000mAh battery was designed and manufactured in order to fit the physical space inside the AUV.



Figure 4.24 Custom Battery Configuration.

4.3.1.8. Thrusters

The motor is designed to operate underwater, an isolation strategy needs to be developed. In this context, 3 main elements needed to be insulated within the motor: Windings, magnets, and silicon steel sheets. If these elements need to be examined in order; The windings are wound using enameled copper cables. These windings are isolated from the siliceous sheet by applying varnish after the winding process. In addition, by covering the windings with epoxy resin, it is aimed to provide insulation against water, which is foreseen to fill into the motor. The magnets are covered with water resistant chrome material. It is foreseen that this coating will protect the magnets against possible corrosion due to working under water. For the insulation of the silicon steel sheets, it is foreseen that an outer housing made of aluminum material is made on the outermost layer of the rotor. After the selected parameters, analyzes of these motors were made. The power-rpm graphs obtained as a result of the analyzes are presented in Figure 4.26.

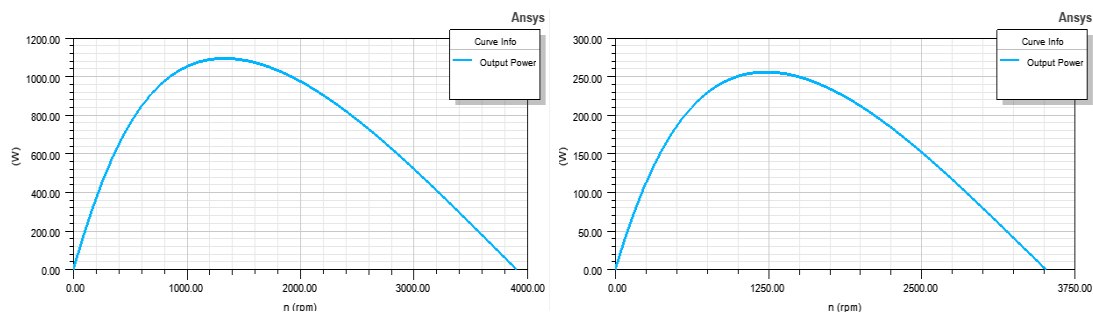


Figure 4.26 Power-Rpm Graphs from Ansys Electronics

It can be obtained from the figure 4.26 that the designed electric motors met their initial values in terms of power-rpm. Even under the stated constraints, more successful designs were obtained than expected. In addition, factors such as torque-speed curve, cogging torque value, efficiency ratio were also taken into consideration. In order to optimize these values, optimization studies were also carried out using the optimetrics plugin included in the Rmxprt plugin, a continuation of the thruster specification is available at section 4.1.2.1 & section 9.5

4.3.1.9. Sensors

A leak sensor has been added inside the AUV in order to indicate any water leakage and shut off the main power so that the vehicle could surface back up. These sensors shown in Figure 4.27. The reason of using a pressure sensor is communicating with Pixhawk to define and holding the depth of the vehicle if needed.

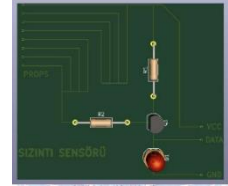


Figure 4.27 Leak Sensor.

4.3.1.10. Acoustic Pinger Locator (APL) Subsystem

With this system, AUV will be able to listen and then determine the location of the underwater beacon, which calls pinger. Using an algorithm based on mathematical analysis and phase analysis of signals emanating from the hydrophone, the companion computer can determine the coordinates of the pinger. This system schemes shown in Figure 4.28 and Figure 4.29.

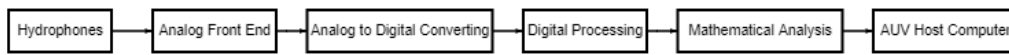


Figure 4.28. General Scheme of APL.

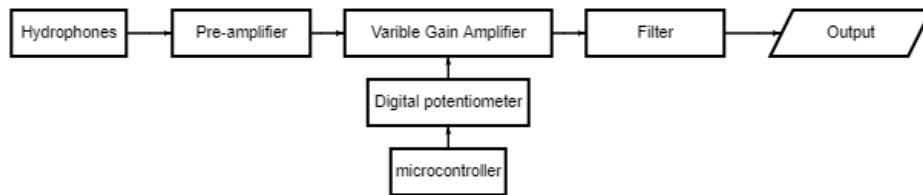


Figure 4.29. General Scheme of Analog Front End.

4.3.1.10.1. Simulation

For simulating amplifier and filter circuit Proteus software was used. In Figure 4.30. output from the board is shown.

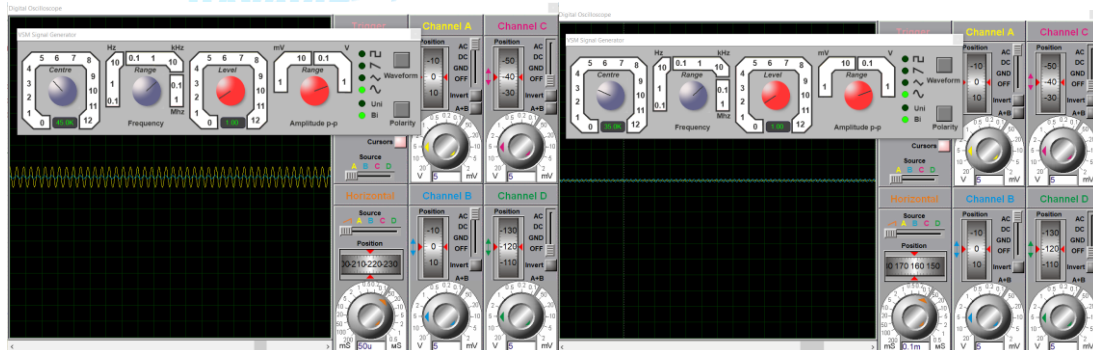


Figure 4.30 Outputs of Required 45kHz Frequency.

STM32F407G-DISCOVERY was used for analog to digital conversion. HAL library has used to write the code and configure the pins of the microcontroller. For writing the code

Cube IDE from ST microelectronics has used. Figure 4.30 shows the code for the analog to digital conversion.

4.3.2. Algorithm Design Process

Flowcharts created for TEKNOFEST 2022 Unmanned Underwater Systems Competition Senior Category are presented in Figure 4.31, Figure 4.32 and Figure 4.33.

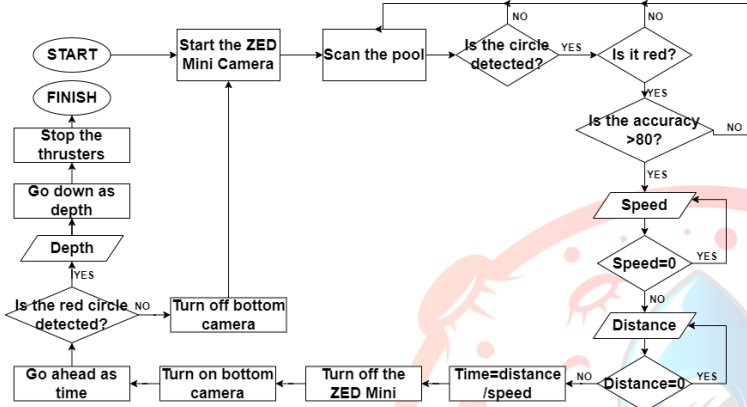


Figure 4.31 Flowchart of Task 1.

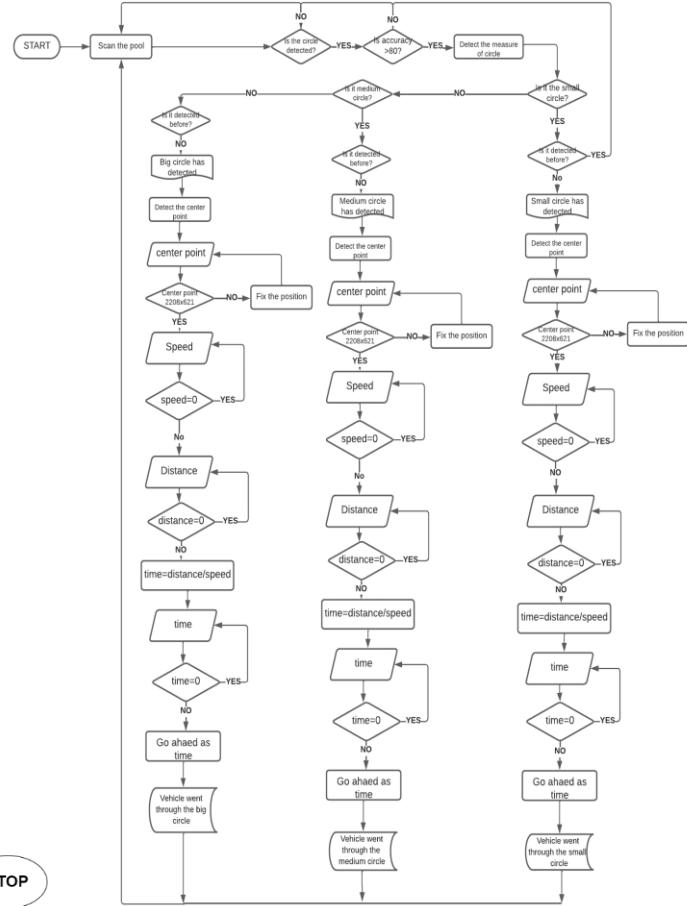


Figure 4.32 Flowchart of Task 2.

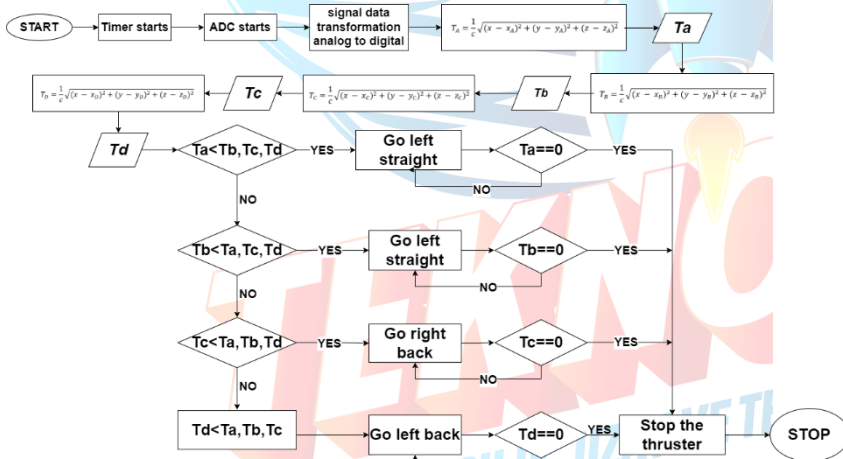


Figure 4.33 Flowchart of Task 3.

As presented in Section 4.3.1.3, a Dual Camera System will be used for Task 1.

4.3.2.1. Vehicle Control

The Python programming language was utilized to build movement function codes and operate the vehicle. The Jetson Xavier NX and Pixhawk communicated using the MAVLink protocol. Pymavlink is a python implementation of the MAVLink protocol. With Pymavlink, it is possible to create a python script to read sensor data and send commands to an ArduSub vehicle. A screenshot of the movement function codes is shown in the Figure 4.34.


```

def forward(t):
    buttons = 1 + 1 << 3 + 1 << 7
    master.mav.manual_control_send(
        master.target_system,
        800,
        0,
        500, # 500 means neutral throttle
        0,
        buttons)
    time.sleep(t)

def backward(t):
    buttons = 1 + 1 << 3 + 1 << 7
    master.mav.manual_control_send(
        master.target_system,
        -800,
        0,
        500, # 500 means neutral throttle
        0,
        buttons)
    time.sleep(t)

def throttleup(t):
    buttons = 1 + 1 << 3 + 1 << 7
    master.mav.manual_control_send(
        master.target_system,
        0,
        0,
        500, # 500 means neutral throttle
        0,
        buttons)

```

Figure 4.34 Autonomous Movement Functions Through Pymavlink.

4.3.2.2. A* Search Algorithm

As mentioned in the Preliminary Design Report, A* Search Algorithm is using in the decision algorithms written by the EVA ROV Team. A* Search Algorithm is basically a searching algorithm that is used to find the shortest path between an initial and a final point. Initially, the algorithm calculates the cost to all its immediate neighboring nodes, n , and chooses the one incurring the least cost. This process repeats until no new nodes can be chosen and all paths have been traversed. Then, it is considered the best path among them. If $f(n)$ represents the final cost, then it can be denoted as:

$$f(n) = g(n) + h(n), \text{ where :}$$

$g(n)$ = cost of traversing from one node to another. This will vary from node to node

$h(n)$ = heuristic approximation of the node's value. This is not a real value but an approximation cost.

Let's explain it with Task 2's weighted graphic. Suppose the AUV is dropped into the pool from position in the weighted graph. According to the task 2, the AUV must pass through all 3 circles only once, regardless of the order. Accordingly, the A* Algorithm does some calculations to reach the smaller circle in the shortest way.

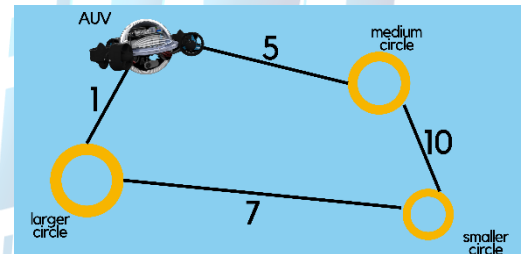


Figure 4.35 Weighted Graph.

Since the start is at the AUV, which will have some initial heuristic value. Hence, the results :

$$f(AUV) = g(AUV) + h(AUV) \quad f(AUV) = 0 + 6 = 6$$

Next, take the path to other neighbouring vertices:

$$f(AUV\text{-}larger\ circle) = 1 + 4 \quad f(AUV\text{-}medium\ circle) = 5 + 2$$

Now take the path to the destination from these nodes, and calculate the weights :

$$f(AUV\text{-}larger\ circle\text{-}smaller\ circle) = (1 + 7) + 0 \quad f(AUV\text{-}medium\ circle\text{-}smaller\ circle) = (5 + 10) + 0$$

It's clear that going through the larger circle first gives us the best path, so this is the node you should use to achieve the destination. Thanks to the A* algorithm, the EVA ROV Team aims to find the shortest path and complete the parkour faster.

4.3.3. Software Design Process

4.3.3.1. Object Detection

It is essential for the AUV to accurately detect targets in order to perform autonomous tasks. It is aimed to correctly evaluate the data received from the camera sensor used. For this purpose, image processing with deep learning methods is planned to use. Works are carried out by EVA ROV Team with YOLO, one of these methods.

YOLO algorithm is a real-time object detection algorithm that offers higher recognition percentage. Unlike the other algorithms, it analyzes the image as a whole after dividing the image sequence into possible parts [5]. The most important feature that distinguishes the YOLOv5 model from other R-CNN, SSD, HOG algorithms is that it processes the image only once, that is, instead of looking at the places where the picture can be found and then detecting the object, it looks at the whole picture once and instantly detects the object. The ability to perform this process simultaneously from the image that it divides in proportions such as 16x16 allows the YOLO algorithm to reach faster and higher prediction rates than other algorithms [5]. The general architecture of the YOLO algorithm is shown in Figure 4.36.

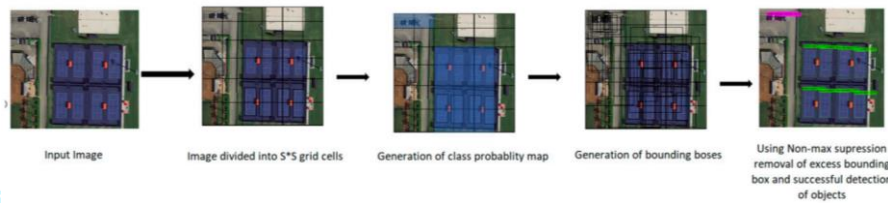


Figure 4.36 General Architecture of YOLO Algorithm.

YOLOv5 is a PyTorch implementation, unlike other YOLO versions. As in YOLOv4 Cross Stage, Partial Networks are used as the backbone and PA-NET is used as the neck [6]. As the activation function, Leaky ReLU and Sigmoid are used. In YOLOv5, the Leaky ReLU activation function is used in the middle/hidden layers and the sigmoid activation function is used in the final detection layer [7]. In YOLO v5, the default optimization function for training is SGD.

A dataset is required for the YOLOv5 algorithm. It is planned by the EVA ROV Team to take original underwater photographs of the task objects in production and add them to the dataset. Apart from this, the photos of the task objects created in the simulation which is presented in Section 4.3.3.2 will also be added to the dataset. Thus, it is aimed to obtain a stronger data set with real and synthetic photographs.

A program called Labellmg is used to label photos. This program allows one or more areas on the images to be labeled as desired. As a result of this tagging, it gives a ".txt" file for each image. Images can be classified thanks to this text file. Labeling of the task objects created in the simulation environment created by the EVA ROV Team on the Labellmg program is presented in Figure 4.37.

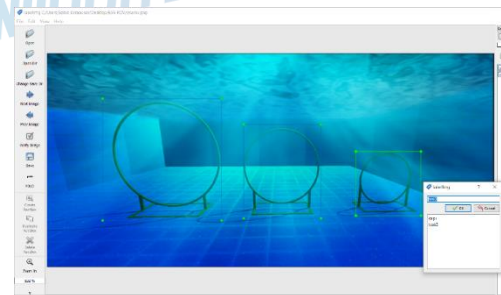


Figure 4.37 Labeling Task Objects of Task.

The colors of photos taken underwater are pale compared to reality. Colors do not reflect reality; most of the time, the blue or green color is too dominant and the colors of the objects in the photo are lost in this intense color distortion. It is important to use a filtration algorithm, especially in order to detect objects of different colors in the 1st task. It is planned to use an algorithm called Sea-Thru in order to transform photographs that have lost their information due to the colors lost by the refraction of light in water, into their real colors.

Sea-thru uses to estimate the distance between the camera and objects in the scene and, in turn, the water's light-attenuating impact [8]. So, photogrammetry is important for this algorithm to be used effectively. An example output of the Sea-Thru algorithm is presented in Figure 4.38.

It is planned to use the Sea-Thru algorithm in order to eliminate the errors that may arise due to the breaking of water in the data set to be prepared.

As mentioned in Section 4.3.1.3, the ZED Mini Stereo Camera is used as a camera sensor in AUV. ZED Mini is a passive depth sensor. Therefore, it can measure depth values at very high ranges.

There are forms of vision with monocular which means one eye and with stereo which means two or more eyes. Stereo cameras provide more precise depth information with left-right photometric alignment compared to monocular cameras [9].

The working principle of depth-sensing with ZED Mini stereo camera is given: A point cloud can be seen as a depth map in three dimensions. While a depth map only contains the distance or Z information for each pixel, a point cloud is a collection of 3D points (X,Y,Z) that represent the external surface of the scene and can contain color information [10, 11].

ZED Mini stereo camera can work underwater. It only needs a camera calibration that needs to be done underwater [12]. An example of calibration in underwater is shown in Figure 4.39.



Figure 4.38 Example Output of Sea-Thru Algorithm.

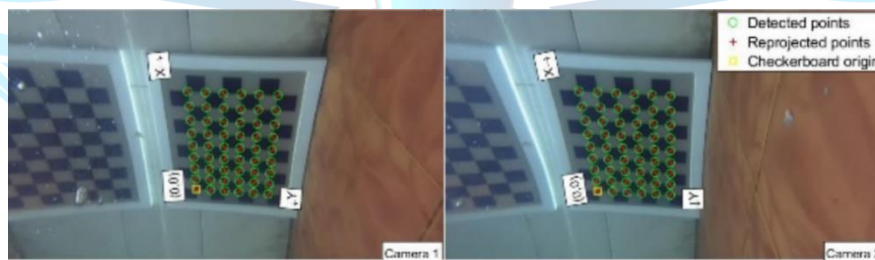


Figure 4.39 The Calibration in Underwater.

The main reason for using the ZED Mini camera is aimed at efficiently measuring the distance of the AUV to underwater objects. ZED Mini stereo camera tests done by EVA ROV Team is presented in details in Section 6.2.

4.3.3.2 Simulation

The first tests made while preparing the autonomous codes of the program were made with Unity. Potential errors that may arise during the competition have been foreseen and corrected on the simulator. Through Unity, tasks that the vehicle will complete during the competition have provided. As a result of the tests, the scenarios that could occur in track environments have identified.

After the simulation environment was fully prepared, firstly, the vehicle was moved in a controlled manner from the outside, and thus the necessary parameters of the vehicle were adjusted. Then, the movement codes prepared for the vehicle were included in the simulation and the codes were tested in the simulation environment, and on top of that, any codes to be made in the codes were included. Notes were taken for the problem and corrected, the final code was uploaded to the test tool and autonomous testing was provided in the real pool. A screenshot of the

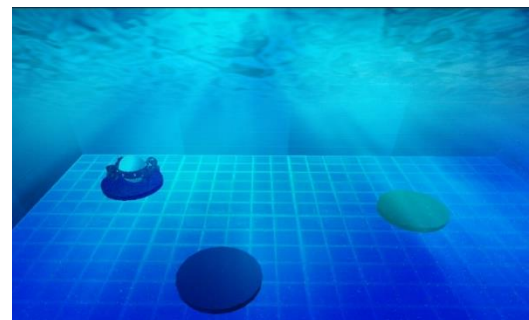


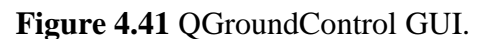
Figure 4.40 A Screenshot of Simulation.

4.4. External Interfaces

Surface control station functionalities are provided by QGroundControl software with Graphical User Interface (GUI) that offers complete flight control and mission planning for the ROV vehicle over the MAVLink protocol. QGroundControl software was used to control and setup the initial PID parameters, sensors and motors before initiating the autonomous testing

Surface control station fu

To operate the Jetson Xavier NX underwater, an ethernet wire was connected between the PC (which runs QGroundControl software) and the Jetson Xavier NX. SSH (The Secure Shell) was used to establish the connection because of the following reasons: The Secure Shell Protocol is a cryptographic network protocol for operating network services securely over an unsecured network. It allows encrypted data transfer and secure communication between the devices.



The emergency switch relay is a safety control switch that prevents overvoltage and current in an electrical circuit and prevents all potential hazards. This key is one of the most important security elements of the vehicle. It is connected in series with the positive pole of the battery and current flows through the switch on the terminal connected in series. The switch acts as a bridge and opens the bridge during an emergency, preventing the current from flowing. The emergency relay that is planned to be used can operate up to 24V and max 40A current values. It is planned to operate the emergency Switch Relay with a zener diode if needed. Some functions of the emergency relay are stopping a movement in a controlled and safe way, monitoring the position of movable guards, a closing transaction interrupt during access, emergency shutdown.



Fuse will be added to the vehicle. Fuses will be fitted to prevent dangerous current levels during charging and discharging. In this context, a 40A fuse and emergency relay, which will meet the needs, will be right next to the driver's panel on land. In this way, the possibility of intervening to the vehicle from the ground in emergency situations will be accelerated.

the rim-driven thruster is a more reliable and safer option than the conventional one, since it has a hub less propeller, that prevents any Nets, algae, or ropes from tangling the motor, which in turn reduces the factors that lead to failure of the thrusters and affects how well the AUV performs, and reduces the risk of human entanglement through hair or fingertips



6. TESTS

Pool tests were done to evaluate and calibrate the movement parameters. Apart from these tests, waterproofing tests was conducted, along side fine tuning the movement parameters, to enhance the accuracy of the movement.

Separate underwater stereo camera tests were done to test and calibrate the accuracy of underwater depth sensing using stereo camera, the tests showed promising results. It was concluded that underwater OpenCV camera calibration with chessboard needed to take place to correct the perspective error caused by the refraction.

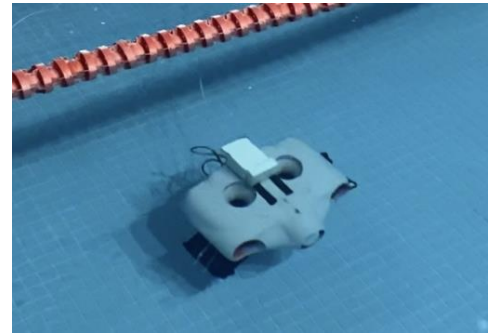


Figure 6.1 Autonomous Underwater Tests.

6.1. Acoustic Pinger Locator (APL) System Tests

To make algorithm work at least 4 hydrophones were needed, so 4 hydrophones were assembled. A test stand has created to test the hydrophones underwater. Hydrophone which were connected to signal generator was simulating pinger on 45kHz frequency. Fast Fourier Transform function has used in the oscilloscope to see the frequency response of the receiving hydrophone. A signal with an amplitude of 100 milivolts has received from the distance of 5 meters. As tests showed amplification of the received signal and filtration is needed to cut off all unwanted frequencies.

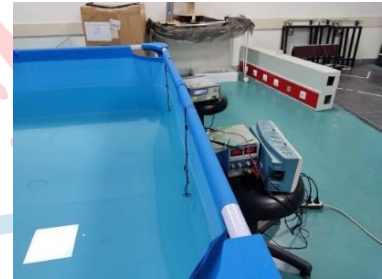


Figure 6.2 Testing Stand.

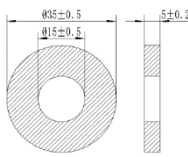


Figure 6.3 JTY21R351505B0-01 Plan.

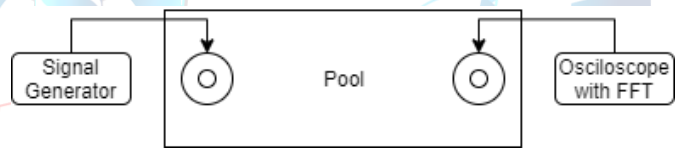


Figure 6.4 Testing Stand Schematic.

6.2. ZED Mini Camera Test

With the work done by the EVA ROV Team, a real-time, depth-measuring model was created with the YOLOv5 algorithm using the ZED Mini stereo camera. Depth codes integrated into YOLOv5 codes are presented in Figure 6.5. The outputs of the model created by the EVA ROV Team are presented in Figure 6.6. It is planned to test the dual camera system created by EVA ROV Team.

```

def main():
    global image_net, exit_signal, run_signal, detections
    capture_thread = Thread(target=capture_thread_func,
                             kwargs={'weights': opt.weights, 'img_size': opt.img_size, 'conf_thres': opt.conf_thres})
    capture_thread.start()
    print("Installing Camera...")
    zed = sl.Camera()
    input_type = sl.InputType()
    if opt.svo != "":
        input_type.set_from_svo_file(opt.svo)
    else:
        input_type.set_from_svo_file(opt.svo)
    # Create a InitParameters object and set configuration parameters
    init_params = sl.InitParameters(input_type=input_type, img_resolution=opt.resolution, img_fps=opt.fps)
    zed_params.camera_resolution = sl.RESOLUTION_1080P
    zed_params.coordinate_system = sl.COORDINATE_SYSTEM_RIGHT_HANDED_Y_UP
    zed_params.depth_mode = sl.DEPTH_MODE_1080P
    zed_params.coordinate_system = sl.COORDINATE_SYSTEM_RIGHT_HANDED_Y_UP
    zed_params.depth_maximum_distance = 50
    runtime_params = sl.RuntimeParameters()
    status = zed.open(init_params)
    if status != sl.ERROR_CODE_SUCCESS:
        print("Error: ", status)
        exit()
    image_left_img = sl.Mat()
    print("Installing Camera")
    positional_tracking_parameters = sl.PositionalTrackingParameters()
    # If the camera is static, uncomment the following line to have better performances and boxes sticked to the ground.
    positional_tracking_parameters.set_sl_static = True
    zed.enable_positional_tracking(positional_tracking_parameters)
    obj_param = sl.ObjectDetectionParameters()
    obj_param.detection_model = sl.DETECTION_MODEL_CUSTOM_BOXES
    zed.enable_object_detection(obj_param)
    objects = sl.Objects()
    obj_runtime_param = sl.ObjectDetectionRuntimeParameters()
  
```

Figure 6.5 Depth Codes Integrated Into YOLOv5 Codes.

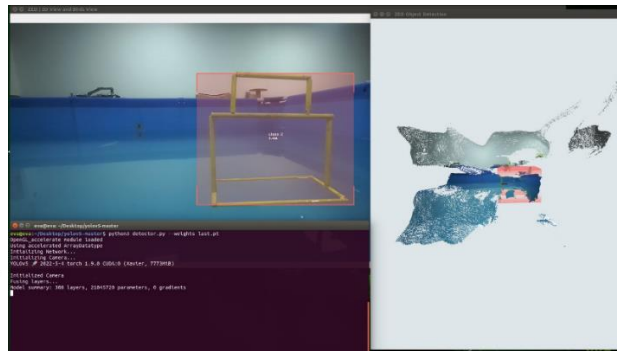


Figure 6.6 The Outputs of the Model.

7. EXPERIENCES

7.1. Mechanical Experiences

An experimental dome was built and put through all the available tests to identify any areas of potential weakness in the design. This was done to guarantee that the final product would be effective. As shown in figure, the screw area breaks when excessive stress is applied to it, therefore it was treated by increasing the fillet between this area and the body.

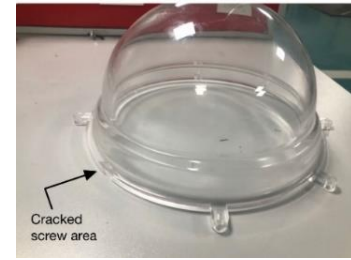


Figure 7.1 A crack in the Screwing Area.

7.2. Software Experiences

Different methods have been tried by the EVA ROV Team for object recognition, which is the most important part of autonomy. One of these methods, examined in four different iterations, runs on the Raspberry Pi 4B card, and three of them run on the NVIDIA Jetson Xavier NX developer kit.

7.2.1 Object Detection Iteration I

YOLOv5 algorithm has used in the object detection iteration I. YOLOv5 is developed in PyTorch framework. Raspberry Pi 4B computer and Raspberry Pi HQ camera have been used to run this model.

7.2.2 Object Detection Iteration II

YOLOv4 algorithm has used in the object detection iteration II. YOLOv4 is developed in Darknet framework. NVIDIA Jetson Xavier NX computer and Logitech C270 camera have been used to run this model. Darknet framework was not suitable for the AUV usecase, since the modified code had to pass on a complex darknet framework in order to get interpreted

7.2.3. Object Detection Iteration III

YOLOv5 algorithm has used in the object detection iteration III. NVIDIA Jetson Xavier NX computer and Logitech C270 camera have been used to run this model. Training took place on GPU. In this model, rotated photos of the gate are also used in case the position of the AUV in the pool changes. PyTorch framework has been used and CUDA was enabled.

7.2.4. Object Detection Iteration IV

YOLOv5 algorithm has used in the object detection iteration IV. NVIDIA Jetson Xavier NX computer and ZED 2 stereo camera have been used to run this model. In object detection iteration IV, depth sensing codes weren't used. Training took place on Google Colab. PyTorch framework has been used and CUDA was enabled.

7.2.5. Conclusion

Table 7.1 Comparative Results of the Iterations.

	Object Detection Iteration I	Object Detection Iteration II	Object Detection Iteration III	Object Detection Iteration IV	Improvement Units	Improvement %
<i>Second per each frame</i>	3 Seconds	0.265 Seconds	0.05 Seconds	0.032 Seconds	-2.95 Seconds	-600.0%
<i>Frame per second</i>	0.33	3.77	16	33	+32 FPS	969.9%
<i>Video resolution</i>	128x98 = 12544Pixel	640x480 = 307200Pixel	640x480 = 307200Pixel	640x480 = 307200Pixel	5X times the Resolution	244.9%
<i>Photos training ration</i>	80+	270+	500+	500+	6.25 X times the photos	62.50%
<i>mAP % (Accuracy)</i>	78%	97%	98%	98%	12% more accurate	12.56%

7.3. Hydrophone Experience

At first version of the hydrophone, available piezoceramic disk Murata 7BB-35-3C was used. The main problems of the first version was insufficient susceptibility to a signal with a 45 kilohertz frequency with narrowly focused signal reception, Coaxial cable for connection was used at first, but then it was decided to change the cable, because the main core of the coaxial cable could split the piezoceramic plate under angular load, The first version of the amplifier was not matching the requirements. OP77 amplifier chip from analogue devices. Since it did not provide significant gain of the signal at 45 kilohertz frequency. Secondly, this operational amplifier uses bipolar power (+12 volts and -12 volts). To assemble an OP77-based amplifier, it had to significantly complicate the design of the amplifier and power supply system.

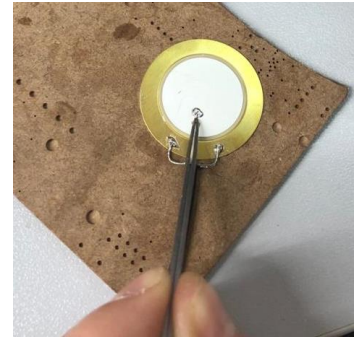


Figure 7.2 The First Version of Hydrophone without Silicone Waterproofing.

8. TIME, BUDGET, AND RISK PLANNING

8.1. Budget Planning

EVA ROV Team's determined budget is 55.000 TL. The expense table made as a result of the budget planning made to realize the project is presented in Table 8.1.

Table 8.1 Budget Planning of EVA ROV Team.

Product	Piece	Price	Total Price
Inductors	40	₺ 8.20	₺ 328
Capacitors	130	₺ 2	₺ 260
Resistors	180	₺ 1.50	₺ 270
Plexiglass Shell	2	₺ 2350	₺ 4700
Zed Camera Mini	1	₺ 7500	₺ 7500
Amplifier	9	₺ 50	₺ 450
Digital Potentiometer Board Module	5	₺ 40	₺ 200
STM Discovery	1	₺ 885	₺ 885
Spray Paint	3	₺ 60	₺ 180
BMS Protected Charger	2	₺ 10	₺ 20
Transistor	10	₺ 5	₺ 50
NVIDIA Jetson Xavier NX	1	₺ 12390	₺ 12390
G-350 ROV Thruster	6	₺ 1.362	₺ 8.173
Lenta Marine ESC	6	₺ 362	₺ 2.173
Battery 5S 5000mAh	1	₺ 1.7820	₺ 1.782
Pixhawk 2.4.8	1	₺ 2665	₺ 2665
O-rings, silica gel, cables, etc..)	-	₺ 250	₺ 250
Pressure sensor	1	₺ 1014	₺ 1014
Weight Set	2	₺ 80	₺ 160
PLA filament 1 kg	3	₺ 181	₺ 543
Switch	1	₺ 157	₺ 157

Digital Potentiometer Integration	1	₺ 50	ultrasonic
Ultrasonic Piezoelectric Elements	5	₺ 70	₺ 350
Ultrasonic piezoelectric elements	4	₺ 10	₺ 40
Piezoceramic Sound Diffuser	20	₺ 10	₺ 200
PCB connector	50	₺ 10	₺ 500
Adjustable Step Up Boost Voltage Booster Regulator Board	2	₺ 20	₺ 40
Relay	10	₺ 20	₺ 200
Waterproof Epoxy	3	₺ 55	₺ 165
10 mm water connectors	8	₺ 35	₺ 280
Switch	1	₺ 157	₺ 157
Pinger/sonar materials (variables amplifier-gain etc...)	-	₺ 2800	₺ 2800
Power distributions	4	₺ 96,52	₺ 386
Waterproof Epoxy	3	₺ 55	₺ 165
Lead weight + CNC		₺ 2500	₺ 2500
10 mm water connectors	8	₺ 35	₺ 280
Total			₺ 52.000

8.2. Time Planning

As a result of the time planning created to realize the project, the working plan is presented in Table 8.2.

Table 8.2 Time Planning.

TO-DO LIST	Mar	Apr	May	Jun	Jul
Body mold production					
Sonar production					
Simulation tests					
Combining all systems and tests					
Body production					
Processing of data in accordance					
Emergency button works					
Completing the mechanical assembly of the vehicle					
Water-resistance improvements					
Tightness and mobility tests					
Final checks, preparations for the competition					
Capability Video Shooting					
Competition					

8.3. Risk Planning

Table 8.3 Risk Planning of the Project.

RISK PLANNING OF THE PROJECT OVERALL	
Risks	Solutions
Water may seep into the electronics box/tube.	Necessary leak tests will be carried out to prevent water leakage and safe working conditions of electronic elements will be provided by supporting them with sealing elements.
There may be a technical malfunction of unknown origin.	The designs will be carefully reviewed and the problem will be simulated.
Financial resources may be insufficient.	The search for sponsors will be continued.
Parts of the AUV in the production process and testing may be deformed.	Routine before each launch of the vehicle is being checked. If a defective part is found, a spare part is installed. Otherwise, part replacement by producing a new one is provided.
The battery may run out and we may not be able to connect with the vehicle.	The vehicle will rise above the water and recharge itself from the solar panels and send us the location information.

9. ORIGINALITY

9.1. Acoustic Pinger Locator (APL) System

In the task, there is a pinger at an unknown distance from the AUV. The duration of its ping, frequency, period are known. It is required to find its location using only passive acoustics. After the sound wave is emitted, the receiver receives the signal, processes and outputs the location in coordinates to the head computer of the AUV.

After the conducted research in the field of localization of acoustic signals, it was decided to use the hyperbolic positioning method, also known as multilateration. Multilateration is a method of determining the position of a stationary or moving object by measuring the arrival time (TOAs) of almost any type (physical phenomenon) of an energy wave with a known waveform and propagation velocity when moving between (navigation) or between (observation) several system stations. This method is widely used in GPS.

This is the mathematical model of multilateration, where (x,y,z) are coordinates of pinger, c is wave propagation and t is the travel time. By multiplying c and t, it gets distance R.

$$ct_i = R_i = \sqrt{(x - x_i)^2 + (y - y_i)^2 + (z - z_i)^2}$$

$$ct_j = R_j = \sqrt{(x - x_j)^2 + (y - y_j)^2 + (z - z_j)^2}$$

$$ct_k = R_k = \sqrt{(x - x_k)^2 + (y - y_k)^2 + (z - z_k)^2}$$

$$ct_l = R_l = \sqrt{(x - x_l)^2 + (y - y_l)^2 + (z - z_l)^2}$$

Computing the solution (x, y, z) is performed by solving the intersections of the hyperboloids. To solve this problem, Fang's (1990) method is used [13]. The full solution is described in Potluri's (2002) work [14]. To find times of arrival of the signal to different hydrophones, cross-correlation method will be used [15].

9.2. Solar Panels

Solar panels are used in the vehicle. The system has created by EVA ROV Team originally is an energy source that contains many solar cells that absorb solar energy on the solar panel. Solar panels convert sunlight into electricity. This Solar Panel shown in Figure 9.1.

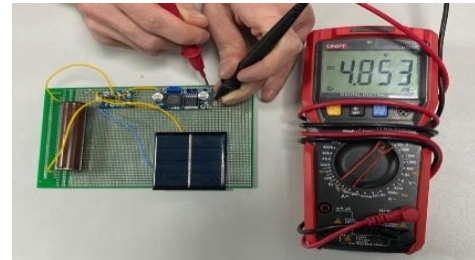


Figure 9.1 Solar Panel LiPo charge Test.

The AUV is designed to reside on the surface while recharging batteries and then to execute its programmed mission. While on the surface the AUV is designed to communicate via Iridium or satellite or RF communications connect to upload collected data and to allow reprogramming of mission profiles. A bi-directional acoustic link provides for data acquisition from underwater instrumentation. Development of the AUV has generated numerous engineering challenges in design of the solar recharge system, design of a propulsion/direction control system capable of handling the unique shape requirement, design of the telemetry system, and development of movement algorithms that include surfacing and battery recharge requirements.

9.3 Remote Communication

As the operation concept, the EVA ROV will surface when the battery of the vehicle runs out, and the Arduino Mega 2560 R3 module receives the location information with the Grove GPS (Air530) module and receives the GPS data from the Arduino GSM Shield 2 module, which works in an integrated way with the EVA ROV Team via the internet. It will be sent to the website designed by the EVA ROV Team and it will inform the team members that the vehicle's battery is dead and the vehicle will return to land.

Position detection is based on the logic of detecting the position of any living or inanimate object. Methods such as GPS and Wi-Fi can be used for location detection. The Grove GPS (Air530) module was preferred because it provides ease of use compared to other modules in location determination with GPS, the data can be easily encoded and it can work in harmony with the module to be used.

Grove GPS (Air530) is a high-performance satellite positioning and navigation module that can be used with Arduino Mega. It supports GPS/Beidou/Glonass/Galileo/QZSS/SBAS and can receive more than 6 satellites simultaneously.

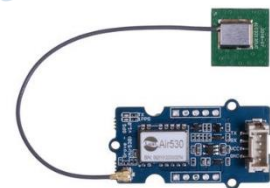


Figure 9.2. Grove GPS (Air530).

Remote communication, in other words telemetry, is the wired or wireless monitoring and optional control of a system. Protocols such as MODBUS, GSM, Bluetooth, LoRaWAN, Zigbee are used for remote communication. The GSM protocol is a protocol that functions and is used as a radio in the structure of mobile phones. Arduino GSM Shield 2 module; It can perform operations such as connecting to the internet, sending SMS, and calling. It has been decided to use the GSM protocol and Arduino GSM Shield 2 module as communication in the EVA ROV Team, since it can be connected to the satellite wherever it can be connected to the satellite during communication to other telemetry modules and the data sent to the internet can be viewed by all other computers.

The GSM Shield 2 module will be used integrated with the Arduino Mega board –shown

in Figure 9.3. The Arduino Mega 2560 R3 board to be used has been decided to be used because it has a higher SRAM size than other Arduino board processors and has more I/O pins.



Figure 9.3 Arduino GSM Shield 2 and Arduino Mega 2560 R3.

The Arduino Mega 2560 R3 board sends the location information it receives from the Grove GPS (Air530) module connected to it at the locations where GPS data is requested, to the website created by the EVA ROV Team with the Arduino GSM Shield 2 module. Incoming data is displayed on the site and a log record of each data is kept. Data transmission is carried out with a frequency of 5 Hz. The data have sent to the server are saved in the database after passing the security check. The recorded data are updated instantly in the user interface. The operating system has preferred for the server is Ubuntu 18.04. Submitted requests to catch and run the webserver have used the ExpressJS module of NodeJS. One of the most important reasons ExpressJS besides being fast and easy, thanks to NodeJS is allowed to easily include many libraries in the project is to provide. Thus, the development process has spent cut the time in half. The User React library has been used to improve the interface, so the entire project is under the umbrella of the NodeJS development process, and the progressive workload is reduced in the process of adding new components , a detailed schematic presented in Figure 9.4

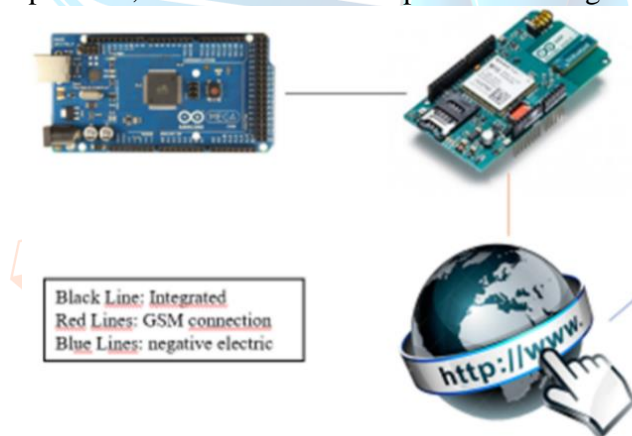


Figure 9.4 GSM Diagram.

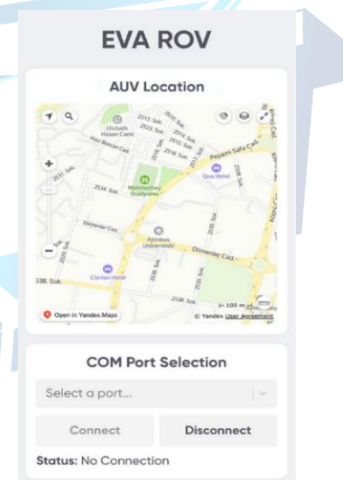

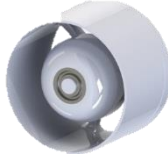


Figure 9.5 Telemetry Application.

9.5 Thrusters

In the competition, "domestication" studies were carried out in the lights of domesticity of the underwater vehicle. The motors has designed and planned in an original way. Designs have been started for the realization that 6 electric motors used in this underwater vehicle in 2 different types. It has been decided that 2 of these motors will be hub less direct current motors and the other 4 will be a traditional outrunner thruster. Since the Hubless motors provide a higher thrust power , but also weight more than a normal thruster External rotor BLDC motors were specifically designed for the AUV use case in mind The power, weight, torque and rpm of these motors are calculated for the tasks.

Table 9.1.The Starting Parameters

	Motor Type	Photo	Outer Diameter (mm)	Inner Diameter (mm)	Power (Watt)	Rpm	Mass (g)
Main Thrusters	Hubless Inrunner BLDC		110	85	600+	3000+	400
Routers	Outrunner BLDC		50	15	200+	2000+	250

The Design and analysis were conducted on the Rmxprt plug-in of Ansys Electronics after the required thruster specifications were determined the motors specifications are presented in Table 9.1, later on an FEA analysis were made in Maxwell program. In order to provide the determined label values, some selected parameters of the mentioned electric motors are presented in Table 9.2.

Table 9.1. Selected Parameters

	Number of Slots	Number of Poles	Magnet Type	Rotor Material	Stator Material	Winding Type	Slot Fill Factor
Main Thrusters	18	20	NdFe35	M330 Silicon Steel	M330 Silicon Steel	Full-Concentric	%28
Routers	12	14	NdFe35	M330 Silicon Steel	M330 Silicon Steel	Full-Concentric	%29

10. DOMESTIC COMPONENTS

10.1. Power Distribution Board

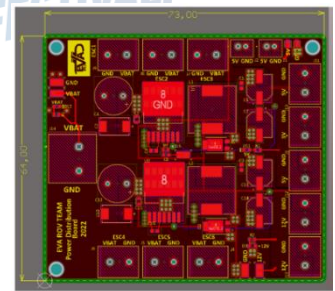
Saturn's electronic design is divided into 3 main units as image processing, motor control, and communication. While NVIDIA Jetson Xavier NX Developer Kit provides communication with the control station and image processing, Pixhawk controls the motor.

Board also has 1 connector for battery input, 6 connectors for ESC output, 2 12 volt output connectors, and 5 5 volt output connectors. In addition, it is resistant to short circuit protection.

EVA ROV Team's board is designed in a 4-layer PCB of 73x64mm in the smallest possible way, providing the highest reliability and high efficiency. Further information is presented in Section 4.3.1.5.

10.2. Acoustic Pinger Locator (APL) System

Sound is a physical effect that represents the propagation of elastic waves in a gaseous, liquid or solid medium. The principle of operation of the microphone is that the pressure of

**Figure 10.1** 2D View of Power Distribution Board.

sound vibrations of air, water or solid matter acts on the thin membrane of the microphone. In turn, the vibrations of the membrane excite electrical vibrations. Piezoelectric effect, the effect of the occurrence of polarization of a dielectric under the influence of mechanical impact. Mechanical impact may occur due to sound. Since the signal emitted by the pinger is ultrasonic, conventional microphones designed cannot be used to receive audible frequencies.

Omnidirectional hydrophones which has a resonant frequency 45 kHz have designed by EVA ROV Team. There are several reasons to choose this component. First of all, the resonant frequency of this component is the required 45KHz. The polarization of this element occurs during transverse deformation. This is important because it allows the hydrophone to be omnidirectional rather than unidirectional.

10.2.1. Variable Gain Amplifier (VGA)

After researches and tests, the LM386 amplifier from Texas Instruments has chosen. The LM386 is power amplifier which were designed for using in low voltage consumer applications. The gain is internally set to 20 to keep external part count low, but the addition of an external resistor and capacitor between pins 1 and 8 will increase the gain to any value from 20 to 200.

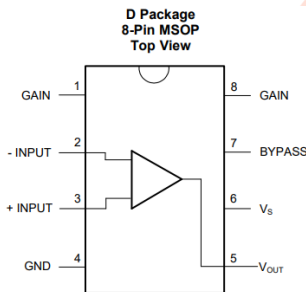


Figure 10.2 LM386 Amplifier Plan.

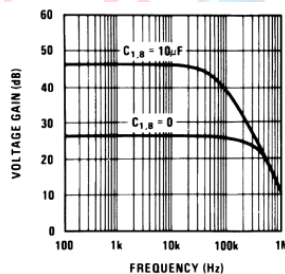


Figure 10.3 LM386 Amplifier Voltage Gain-

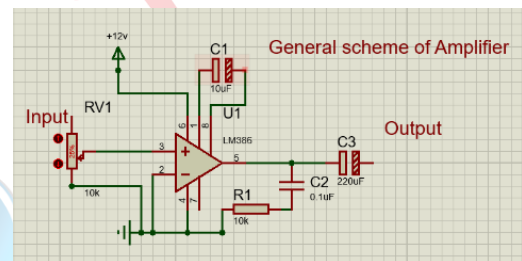


Figure 10.4 Amplifier Schematic.

This amplifier is suitable for us because it can effectively amplify the signal at a frequency of 45KHz. Also the gain of the amplification which is important for the task can be changed.

10.2.2. Digital Potentiometer

The main amplifier must be dynamically configurable so that at large distances it is possible to see small attenuated signals due to the loss of signal power propagating in the water, but when the system is close to the signal source, so that the amplifier does not saturate, it reduces the gain. Since the value of the potentiometer to control the gain underwater can be changed, using the digital potentiometer has decided. X9C10 chip from Renesas is used to change the gain of the amplifier.

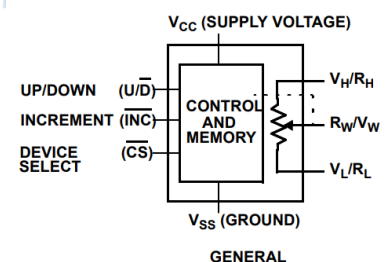


Figure 10.5 X9C10 Chip Plan.

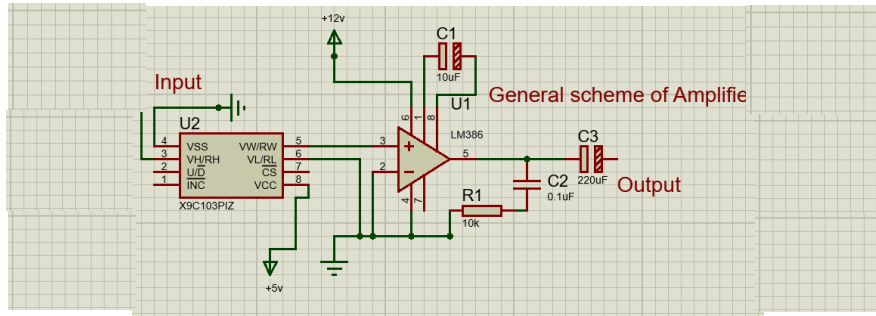


Figure 10.6 X9C10 Chip with Amplifier Schematic.

The resistance is controlled through UP/DOWN, INCREMENT and CS pins. STM32F407G DISCOVERY is used to control it.

10.2.3. Filter

A second order Butterworth bandpass filter has designed by EVA ROV Team to filter the signal from unwanted noise.

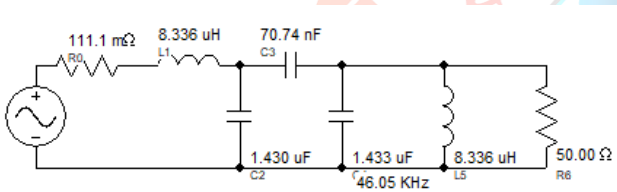


Figure 10.7 Filter Schematic.



Figure 10.8 Filter.

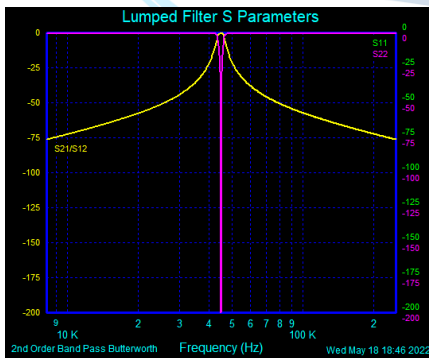


Figure 10.9 Filter Characteristics.

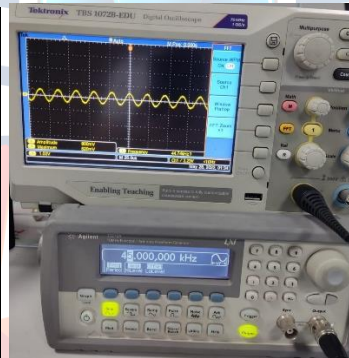


Figure 10.10 Amplified Output of the Board with Filter on Required 45kHz Frequency.

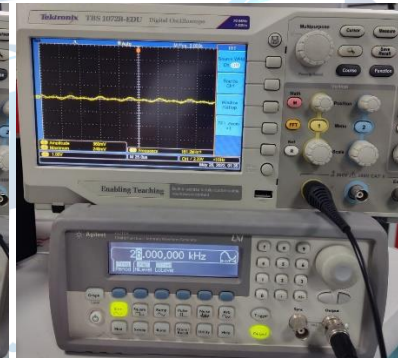


Figure 10.11 Amplified Output of the Board with Filter on Another Frequency which the Filter Filtered.

10.3 Electric Speed Controller

An electronic speed controller has designed and manufactured by EVA ROV Team for BLCD motor driver which can run from 15 to 36 volt and maximum current it can handle 30 amp. It uses six step commutation method to drive motor. It has 3 main part these are microprocessor, voltage regulation, power and back emf sensing, the technical details have been presented in Section 4.3.1.4.

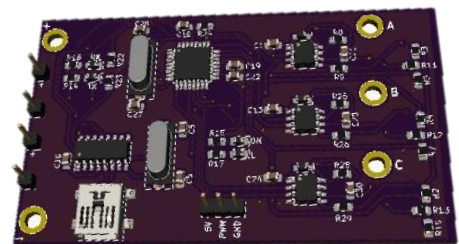


Figure 10.12 Electric Speed Controller Board.

11. REFERENCES

- [1] Eldred, R., & Van Bossuyt, D. L. (2022). Preliminary Design and Testing of a Resetting Combination Anchor, Antenna, and Tether Mechanism for a Spherical Autonomous Underwater Vehicle. *Applied Sciences*, 12(10), 5072.
- [2] Suarez Fernandez, R. A., Parra R, E. A., Milosevic, Z., Dominguez, S., & Rossi, C. (2019). Nonlinear attitude control of a spherical underwater vehicle. *Sensors*, 19(6), 1445.
- [3] Yue-lin Zhang, Jian Jin, Hai-liang Hou, Shu-yong Liu, Xiu-lei Wei, The buckling strength of plexiglass protective shield under static water pressure, *Engineering Failure Analysis*, Volume 99, 2019
- [4] Dong, Y. (2002). Effects of material properties and numerical simulation on thermoforming acrylic sheets (Doctoral dissertation, University of Auckland).
- [5] Nepal, U., & Eslamiat, H. (2022). Comparing YOLOv3, YOLOv4 and YOLOv5 for Autonomous Landing Spot Detection in Faulty UAVs. *Sensors*, 22(2), 464. <https://doi.org/10.3390/s22020464>
- [6] Yu, Y., Zhao, J., Gong, Q., Huang, C., Zheng, G., & Ma, J. (2021). Real-Time Underwater Maritime Object Detection in Side-Scan Sonar Images Based on Transformer-YOLOv5. *Remote Sensing*, 13(18), 3555. <https://doi.org/10.3390/rs13183555>
- [7] Xu, Qingqing & Zhu, Zhiyu & Ge, Huilin & Zhang, Zheqing & Zang, Xu. (2021). Effective Face Detector Based on YOLOv5 and Superresolution Reconstruction. *Computational and Mathematical Methods in Medicine*. 2021. 1-9. 10.1155/2021/7748350.
- [8] D. Akkaynak and T. Treibitz, "Sea-Thru: A Method for Removing Water From Underwater Images," 2019 IEEE/CVF Conference on Computer Vision and Pattern Recognition (CVPR), 2019, pp. 1682-1691, doi: 10.1109/CVPR.2019.00178.
- [9] Dandil, E., & ÇEVİK, K. K. (2019, October). Computer vision-based distance measurement system using stereo camera view. In 2019 3rd International Symposium on Multidisciplinary Studies and Innovative Technologies (ISMSIT) (pp. 1-4). IEEE.
- [10] *Depth Sensing Overview*. Stereolabs. <https://www.stereolabs.com/docs/depth-sensing/>
- [11] Ortiz, L. E., Cabrera, V. E., & Goncalves, L. M. (2018). Depth data error modeling of the ZED 3D vision sensor from stereolabs. *ELCVIA: electronic letters on computer vision and image analysis*, 17(1), 1-15.
- [12] C. Wang et al., "Research and Experiment of an Underwater Stereo Vision System," OCEANS 2019 - Marseille, 2019, pp. 1-5, doi: 10.1109/OCEANSE.2019.8867236.
- [13] B.T. Fang, (1990). *Simple solutions for a hyperbolic and related position fixes*, IEEE Trans. on Aerosp. and Elect. Systems, vol. 26, no. 5, pp. 748-753.
- [14] S. Potluri, (2002). *Hyperbolic position location estimator with TDOAS from four stations*. Published master's thesis, New Jersey Institute of Technology, USA.
- [15] A.I. Mashoshin (2019). *Algorithm for determining the coordinates of the underwater acoustic source using the correlation function of its signal*. JSC "Concern "Central Research Institute "Electropribor", Russia.